Virtual-Cathode Oscillator Emission by a Pinched Diode

J. Benford, H. Sze, W. Woo, and B. Harteneck
Physics International Company, San Leandro, California 94577
(Received 29 July 1985)

Pinched electron beams emit high-power microwaves by formation of a virtual cathode. Radiation occurs simultaneously with pinching or slightly thereafter. Observations of strong electrostatic fields and the partitioning of current into reflexing and transmitting populations at the same time that microwaves are emitted indicate virtual-cathode formation. Microwaves originate mainly from the virtual-cathode side of the anode. Addition of an axial magnetic field suppresses microwave radiation by inhibition of pinching.

PACS numbers: 52.75.Pv, 41.80.Dd, 85.10.Ka

In recent years virtual-cathode oscillators (vircators) have been demonstrated to emit short pulses of very high-power microwaves (up to 4 GW).[1-8] The mechanisms for the emission of this radiation have been attributed to both space and time oscillations of the virtual cathode and the oscillation of electrons in the potential well between the real and virtual cathodes (reflexing). Simulations show both mechanisms occurring simultaneously in some diodes.[8,9] A clear separation of these mechanisms has not been made experimentally, nor has the time history of the formation of the virtual cathode been observed.

We report the observation of high-power microwave radiation with a pinched electron beam. Experimental evidence of simultaneity of onset of electron reflexing, indicating formation of a virtual cathode, and high-power emission is presented. The time history of the beam dynamics and microwave emission are described. Our results clearly demonstrate that the dominant radiation source is on the virtual-cathode side of the anode. Addition of an axial magnetic field suppresses microwave radiation at the field at which pinching ceases.

The virtual cathode is formed inside a 12.7×6.4-cm^2 rectangular waveguide which is 350 cm long and terminated in one end with a movable stub and at the other end with a rectangular horn antenna (Fig. 1). The waveguide has two opposite side-wall openings on its long dimensions located 15 cm from the terminated end. The anode assembly is mounted on one opening. The beam is emitted from a 5.1-cm-diam planar cathode through the anode of 2.5×10^{-3}-cm aluminum foil. As the beam entered the waveguide through the anode, a virtual cathode formed in the waveguide. The rectangular opening on the far side is connected to a rectangular drift chamber with a movable graphite disk on its end wall which serves both as a moving boundary for the virtual cathode and as a current collector. This chamber is $12.7\times12.7\times20$ cm^3.

Current flow in the virtual-cathode experiment was monitored by three self-integrating Rogowski coils. I_T monitored diode current on the real-cathode side of the anode, I_{VC} the current on the virtual-cathode side of the diode, and I_{DS} the current in the downstream drift chamber. Diode voltage V_D was obtained by inductive correction of a resistive voltage monitor locat-

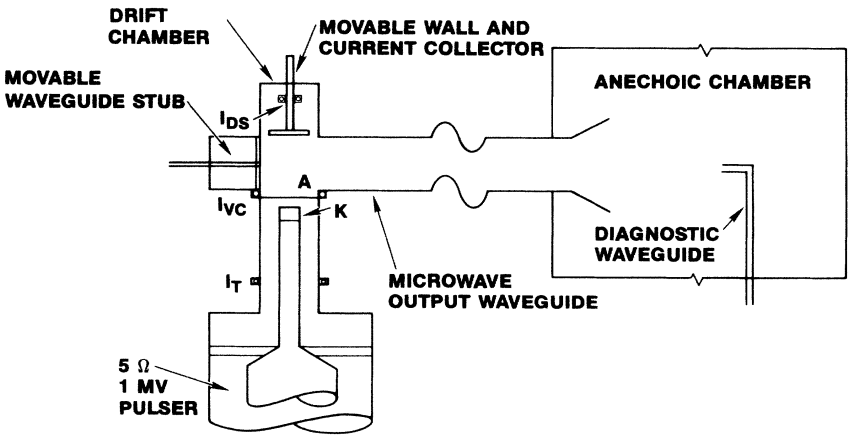

FIG. 1. Schematic diagram of the experimental apparatus.

ed on the water side of the water-vacuum interface. Emission frequencies were measured by a system of coupler, bandpass filter, and crystal detector and an X-band dispersive line. All crystal detectors operated at about 10 mW. The saturation power level was >100 mW. All diagnostic cables (electrical and microwave) were pulsed with a 1-ns pulser to determine cable length. In addition, a fiducial was superimposed on all signals to account for oscilloscope time drift.

Typical voltage, currents, and microwave pulses are shown in Fig. 2. The radiation chirps [Fig. 2(d)], i.e., the frequency increases during the pulse with maximum power occurring at some specific frequency. This central frequency can be altered by a change in the anode-cathode gap. The total power integrated over the far field was approximately 350 MW. The microwave emission was insensitive to the position of the movable waveguide stub. No significant difference was observed between 0.25-, 0.5-, and 1-mil aluminum anodes and a 1-mil aluminized Mylar anode. We observe that radiation always occurs at an inflection point in the current. High-power radiation begins when the diode pinches (Fig. 3), i.e., when the diode magnetic self-field turns electrons through 90° when they cross the gap.[10] The diode follows Child-Langmuir behavior until $I_{CL}=I_c$, the critical current for pinching.[11] The diode then operates at roughly constant voltage as the current increases, which is an indicator of electron reflexing. The radiation peak occurs at current in excess of I_c and below I_p, the parapotential current,[11] at which the pinch flow is fully developed. This observation of microwave radiation from a pinched flow contradicts particle-in-cell simulations which predict suppression of radiation.[8]

I_{VC} measures current propagating through the virtual cathode and returning to ground through the waveguide walls. Current which is reflected from the virtual cathode and reflexes in the anode (I_R), returning to ground through the anode, is not seen by I_{VC}. I_T measures total beam current. Therefore, we measure reflexing current from the partitioning of currents $I_R=I_T-I_{VC}$ [Fig. 2(b)]. Divergence between the two currents is simultaneous with the emission of microwaves and the pulse spike I_{DS} [Fig. 2(c)]. The I_{DS} pulse is electrostatic pickup, i.e., it does not invert when the Rogowski coil is inverted. We interpret this as detection of the strong electric fields from the virtual cathode. As much as one-third of the current returns to ground by reflexing in the anode, and the rest goes through the virtual-cathode region. Partitioning of currents at the same time as the microwave emission is a direct measurement of formation of the virtual cathode.

I_T and I_{VC} diverge at a current higher than theoretical predictions of the current required for virtual-cathode formation.[11] In our experiment, virtual-cathode formation and emission of high-power microwaves occur at ~ 60 kA. The theoretical 1D space-charge limited current for this geometry is ~ 10 kA. The 1D theoretical prediction is invalid for a pinched diode, which is a strongly 2D phenomenon.

In order to determine the mechanism for the generation of the radiation we investigated the configuration shown in Fig. 4. The virtual cathode forms in a region which is inaccessible to the overmoded waveguide. Only radiation from reflexing electrons will propagate into the anechoic chamber. By making openings in the anode at B (Fig. 4) we verified that the

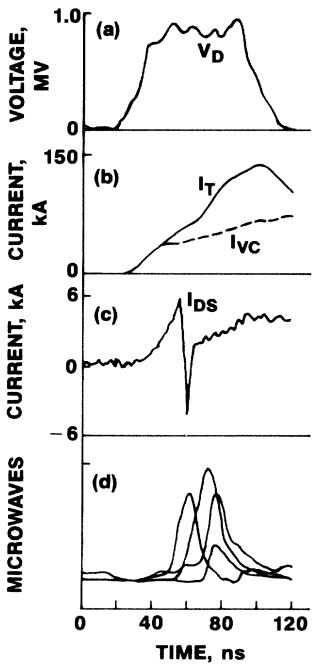

FIG. 2. Typical traces for (a) corrected voltage V_D, (b) total current I_T and propagating current I_{VC}, (c) downstream current I_{DS}, and (d) microwaves with frequency bands 8-9, 9-10, 10-11, and 11-12 GHz, occurring sequentially in time.

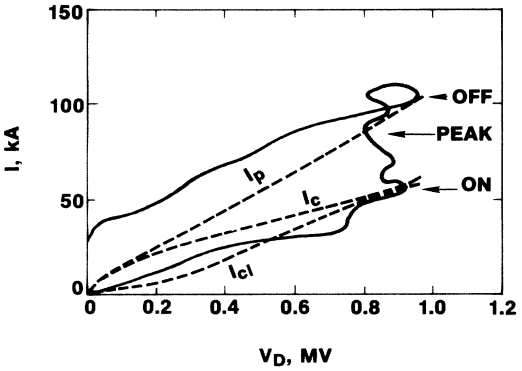

FIG. 3. Typical current as a function of voltage (solid line), and computed values of I_{CL}, I_c, and I_p.

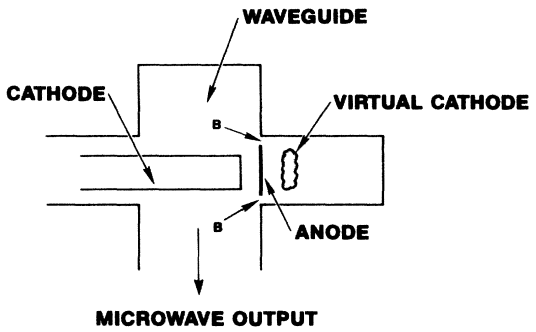

FIG. 4. Schematic diagram of the experimental configuration to determine radiation regions.

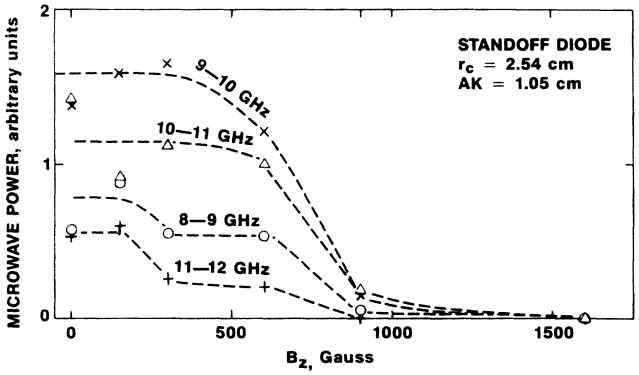

FIG. 5. Microwave suppression by axial guide field.

virtual cathode formed: Substantial radiation leaked into the waveguide. However, when these openings were closed off, the measured radiation was reduced −8.2 dB. Therefore the principal radiation was produced on the virtual-cathode side of the anode, and the contribution from reflexing electrons was small. These results demonstrate that the radiation was produced almost entirely from the oscillating virtual cathode. For the oblique angles of incidence which pinched flow produces, few transits of the anode are expected. Simulations predict little reflexing radiation in such conditions.[8]

Other evidence that pinching is associated with the onset of microwaves comes from the reduction and elimination of microwaves in all bands upon application of an axial magnetic field, attributed to prevention of pinching (Fig. 5). According to the model of Forster,[12] pinching is prevented by a field $B_z = dI_c/r_c^2 c$, where r_c is the cathode radius and d the anode-cathode gap. For this experiment, the predicted field is 1 kG, which is the field at which microwaves are observed to cease. Simulations of the effect of guide field contradict this result. In some cases calculations predict enhanced microwave emission with guide field.[13] Sullivan[14] has suggested that a guide field enhances streaming instabilities which suppress microwave emission.

In summary, early in the pulse the electron beam follows Child-Langmuir behavior. As the beam current approaches the critical current for pinching, electron trajectories are increasingly deflected by the magnetic field on both sides of the anode. At the critical current, the beam pinches along the anode plane, and the virtual cathode forms. The electron population divides into propagating and reflexing parts. High-power microwave radiation and strong electrostatic fields are observed at this time. After ≤ 40 ns, microwave radiation ceases, and the beam continues to propagate. Cessation may be due to ion injection from the heated anode.

We wish to acknowledge the expert assistance of Al York in engineering design and construction of the apparatus, Ron Courtney for experimental operation, and David Bromley for data processing. We are grateful to John Creedon for valuable discussions. This work was supported by the U.S. Defense Nuclear Agency.

[1]R. A. Mahaffey, P. Sprangle, J. Golden, and C. A. Kapetanakos, Phys. Rev. Lett. **39**, 843 (1977).

[2]H. E. Brandt, A. Bromborsky, H. B. Burns, and R. A. Kehs, in *Proceedings of the Second International Topical Conference on High Power Electron and Ion Beam Research and Technology* (Cornell Univ. Press, Ithaca, N.Y., 1977), Vol. 11, p. 649.

[3]A. N. Didenko, G. P. Fomenko, I. Z. Gleizer, Ya. E. Krasik, G. V. Melnikov, S. F. Perelygin, Yu. G. Shtein, A. S. Sulakshin, V. I. Tsvetkov, and A. C. Zerlitsin, in Proceedings of the Third International Topical Conference on High Power Electron and Ion Beam Research and Technology, Novosibirsk, U.S.S.R., 1979 (unpublished), p. 683.

[4]A. N. Didenko, Ya. E. Krasik, S. F. Perelygin, and G. P. Fomenko, Pis'ma Zh. Tekh. Fiz. **5**, 321 (1979) [Sov. Tech. Phys. Lett. **5**, 128 (1979)].

[5]C. Clark, private communication.

[6]H. Sze, J. Benford, T. Young, and D. Bromley, IEEE Trans. Plasma Sci. **13**, 492 (1985).

[7]R. R. Bartsch and H. A. Davis, Bull. Am. Phys. Soc. **29**, 1179 (1984).

[8]S. Burkhardt, R. Scarpetti, and R. L. Lundberg, J. Appl. Phys. **58**, 28 (1985).

[9]T. J. T. Kwan, Phys. Fluids **27**, 228 (1984); B. G. DeVolder, L. E. Thode, G. M. Snell, and T. J. T. Kwan, Bull. Am. Phys. Soc. **29**, 1283 (1984).

[10]Figure 3 is a plot of current I_T vs diode voltage V_c at 1-ns intervals. Both I_T and tube voltage were collected with Tektronix 7912 AD programmable digitizers and then programmed to plot I_T vs V_c at desired time intervals.

[11]R. B. Miller, *An Introduction to the Physics of Intense Charge Particle Beams* (Plenum, New York, 1982), p. 31.

[12]D. W. Forster, "High Current Electron Beam Acceleration in the Presence of an External Magnetic Field: Field Magnitude Criteria," Atomic Weapons Research Establishment Internal Report, 1974 (unpublished).

[13]T. J. T. Kwan and L. E. Thode, Phys. Fluids **27**, 1570 (1984).

[14]D. Sullivan, private communication.

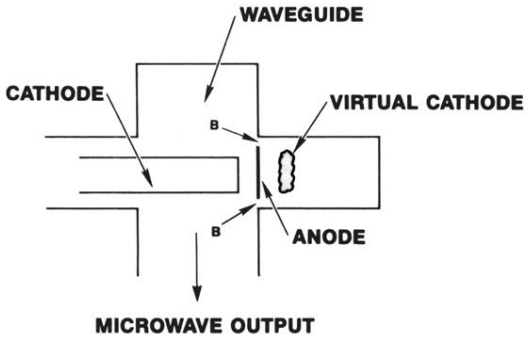

FIG. 4. Schematic diagram of the experimental configuration to determine radiation regions.